

Angular Distributions of Ejected Particles from Ion-Bombarded Clean and Reacted Single-Crystal Surfaces

Nicholas Winograd^(a) and Barbara J. Garrison

Department of Chemistry, Purdue University, West Lafayette, Indiana 47907

and

Don E. Harrison, Jr.

Department of Physics and Chemistry, Naval Postgraduate School, Monterey, California 93940

(Received 22 May 1978)

The expected angular distributions of ejected particles from ion-bombarded clean and reacted single-crystal surfaces are calculated using classical dynamics to model the momentum dissipation. For oxygen atoms adsorbed on a Cu(100) lattice in *A*-top and fourfold and twofold bridged geometries, preferred ejection angles are found for the higher-kinetic-energy particles (>20 eV). Because of scattering mechanisms which cause atoms to move through gaps in the lattice surface, we find that the patterns for different overlayer registries are easily distinguishable.

The determination of site positions of adsorbates on single-crystal surfaces is a central problem in the construction of bonding schemes to describe chemisorption. In this Letter we report the first full molecular dynamical calculations of ejected-atom angular distributions for ordered overlayers on metal surfaces subjected to 600-eV Ar⁺-ion bombardment. We find that when adsorbed atoms are placed in specific orientations with respect to the lattice holes, various registries of these layers can be distinguished with high precision. We present the angular distributions from clean metal surfaces which have been observed experimentally,¹⁻³ and the predicted distributions when oxygen atoms are adsorbed in twofold and fourfold bridge sites and in *A*-top sites on a Cu(100) surface. In addition, we establish for the first time the scattering mechanisms that give rise to these angular distributions. These mechanisms are conceptually straightforward in that the scattering of the ejected atom is directed through the gaps in the lattice surface.

The angular distributions of the ejected particles in our calculations were determined using classical dynamics. This procedure allows the positions and momenta of all the particles to be determined as the momentum of the primary ion dissipates throughout the crystal. The details of the method including the integration scheme,^{3,4} the bulk-solid potential,^{4,5} and the ion-solid potential⁵ have been described previously. The model microcrystallite consists of four square layers with approximately sixty atoms per layer, a size which is large enough to contain all of the atomic motion that gives rise to particle ejection.⁶ The trajectories reported here were computed

using 600-eV Ar⁺-ion bombardment at normal incidence to one of the three low-index faces of copper. For each case, approximately 100 different impact points were chosen which were regularly distributed over a zone of irreducible surface symmetry. The angular distributions could then be found by appropriately unfolding this zone so that it completely encompassed the target atom.³

The adsorbate atoms were placed in a *c*(2×2) array above the Cu(100) surface plane. Since appropriate pair potentials for CuO are unavailable, we have assumed a form similar to the copper potential with a binding energy adjusted to yield a reasonable adsorption energy. The oxygen-oxygen interactions are included in a similar manner. The heights above the surface for the *A*-top site and for the fourfold and twofold bridge sites were calculated from their equilibrium separation distance⁶ to be 2.55, 1.74, and 2.13 Å, respectively. These configurations are shown in Fig. 1.

The calculated angular distributions of ejected atoms from the clean Cu(100), Cu(110), and Cu(111) surfaces are shown in Figs. 2(a)–2(c). Note that both the fourfold symmetry exhibited by the (100) face and the polar deflection angle of 44° are in precise agreement with experimental studies.⁷ The nearly sixfold symmetry found on the (111) face and the diffuse rectangular pattern on the (110) face are in qualitative agreement with experimental results.^{1,2,8} Of more interest, however, is that by selecting only those particles with rather high kinetic energy, >20 eV, the fraction of particles ejected along preferred crystallographic directions is consider-

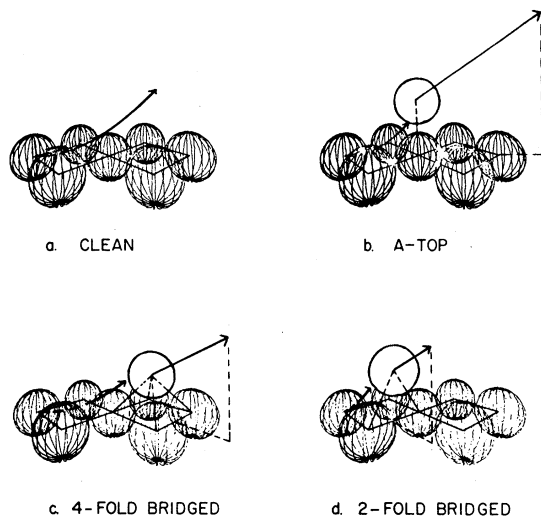


FIG. 1. Schematic representation of the (100) surface with adsorbed oxygen shown in its A-top site and its twofold and fourfold bridged site. The arrows indicate the preferred scattering directions for each case. The atomic radii are drawn to a scale which indicates the distance where repulsive interactions begin. The dotted lines give the projection onto the surface plane of the direction of ejection of the adsorbed oxygen in each case.

ably enhanced as shown in Figs. 2(d)–2(f). The lower-energy particles tend to have a diffuse angular distribution since they are ejected late in the trajectory when much of the surface order is no longer present.

Tracing individual atomic trajectories yields a clear picture of the important scattering mechanisms in the high-kinetic-energy regime. First, most of the ejected particles plotted in Figs. 2(d)–2(f) arise from within two or three lattice spacings from the impact point and suffer only a few scattering events. Second, the spacings between the surface atoms exert a strong directional effect during ejection. The fourfold holes on the (100) face, for example, constrain the path of the ejected atoms, and their trajectories proceed, on the average, in the (001) plane perpendicular to the surface as shown schematically in Fig. 1(a). The same mechanism is applicable to the (111) face; the three elongated lobes arise from scattering through the threefold holes on the crystal surface that do not have second-layer atoms directly under them. In all cases, the atoms ejected from the microcrystallite originate from the top layer. Less angle-resolved structure is ob-

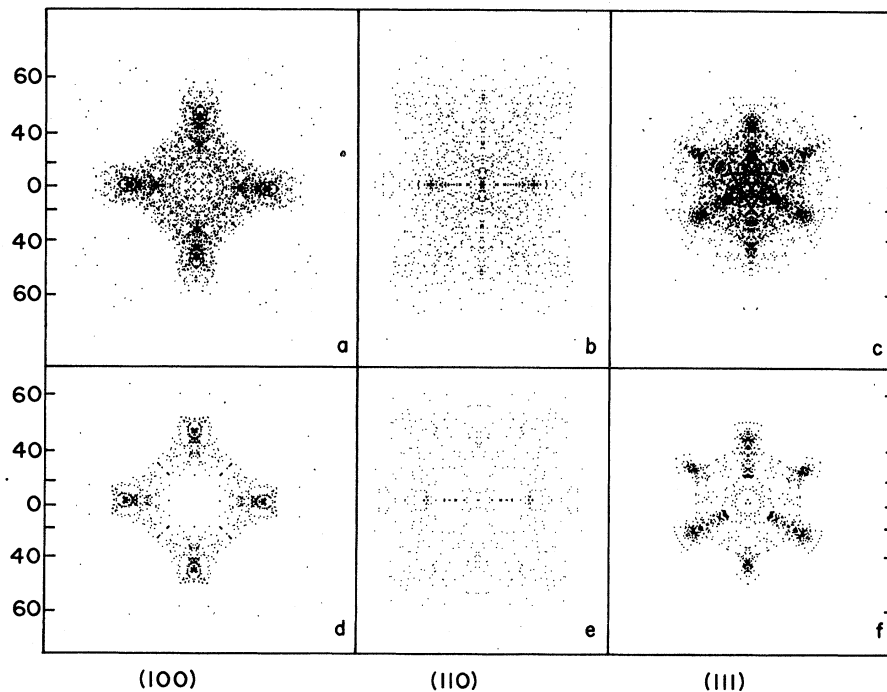


FIG. 2. Angular distributions of ejected particles for the (100), (110), and (111) orientations. Each ejected atom is plotted on a flat-plate collector an arbitrary distance above the crystal. (a)–(c) All ejected particles; (d)–(f) only those atoms whose kinetic energy is greater than 20 eV. The numbers on the ordinate refer to the polar deflection angle given in degrees.

served for the (110) orientation since the rows in the [100] direction are sufficiently far apart to allow the atom to escape at virtually any angle.

Since the lattice surface structure dominates the ejection angle of faster-moving particles, it appears logical that blocking the preferred ejection directions with adsorbed atoms should have a strong effect on the angular distributions. To test this idea we have performed calculations using an adsorbate with the mass of oxygen placed in the specific geometries shown in Fig. 1. The resulting angular distributions for the ejected oxygen atoms and copper atoms are shown in Fig. 3. Note that the distributions of the substrate copper atoms maintain their basic symmetry although the presence of the *A*-top oxygens narrows the patterns while the bridged oxygens broaden them slightly. Of particular interest is that the oxygens themselves show definite preferred ejection angles. Specifically, for the *A*-top config-

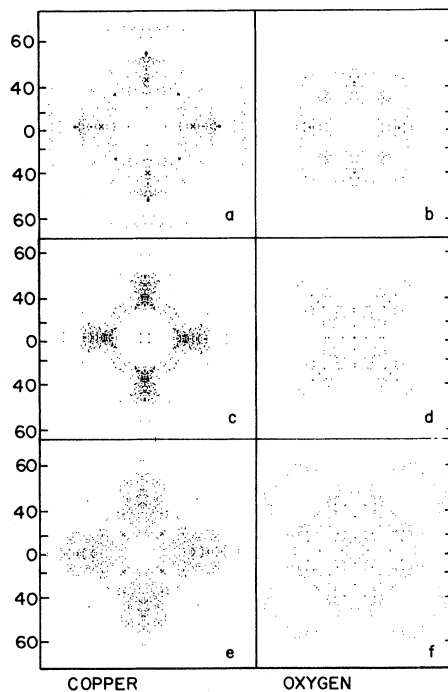


FIG. 3. Angular distributions for the copper and oxygen originating from a $c(2 \times 2)$ structure with oxygens in (a) and (b) an *A*-top, (c) and (d) a fourfold bridge site and (e) and (f) a twofold bridge site. The kinetic energy of the copper atoms is >20 eV for each case, while the kinetic energy for the oxygen atoms is between 20 and 50 eV. The binding energy for oxygen on copper is arbitrarily assumed to be 0.75 eV. The numbers on the ordinate refer to the polar deflection angle given in degrees.

uration, their ejection angles have the same symmetry as the substrate although some weak emission is observed with a symmetry rotated by 45° . Both bridged configurations, however, show a fourfold symmetry rotated by 45° with respect to the substrate. The twofold bridge site shows lobes which are considerably broader than the fourfold bridge site. All three geometries are easily distinguishable.

The mechanism behind these angular distributions concurs with the scheme developed to understand the ejection angles of particles from clean surfaces. For the *A*-top geometry the scattering of the oxygen atom is usually directed by a substrate atom which is being ejected, with both moving off in the same direction. In addition, our analysis shows that the overlayer itself induces some focusing of the ejected particles. This effect is responsible for the narrowing of the copper angular distributions and the weak oxygen fourfold pattern which is rotated by 45° with respect to the substrate.

For the oxygens in bridged geometries the presence of the substrate has a markedly different effect on the ejection angles. When the oxygen atom is placed in a fourfold bridge site it is forced to eject through the valley created by two touching copper atoms. Since the oxygen is closest to the surface plane for this configuration, the ejection angles are particularly well defined. A similar mechanism applies to the twofold bridged oxygen, although the allowed ejection angle is considerably broader since the oxygen atom is further from the surface. For example, we found that only about 80% of the particles eject through the fourfold lattice hole while 20% eject directly over the adjacent substrate atom. These processes are shown schematically in Fig. 1.

The simplified scattering mechanism we have discovered for the atom-ejection process is most strongly influenced by the spatial registry of the adsorbate with respect to the substrate. The patterns are remarkably insensitive to variations in any of the chosen interaction potentials,⁹ and should be observable for a wide variety of systems including molecular adsorbates. Preliminary studies also suggest that tuning of the energy window for the ejected atoms provides an additional check for a specific registry.⁹ Measurement of the angular distribution of ejected particles should prove to be an excellent complement to low-energy electron diffraction—a tool which is very sensitive to the scattering potential and very insensitive to the adsorbate registry¹⁰—and

to angle-resolved photoemission which has proved useful in elucidating molecular geometries on surfaces.¹¹ The angular distributions of electron-stimulated desorbed fragments¹² offer a close parallel to our method, although the mechanism for this case is quite different and the theory still needs further development.¹³

Finally, for the specific case reported here, we believe that the experimental studies can be appropriately carried out using the static mode of secondary ion mass spectrometry¹⁴; the low dose rates of primary ions used with this technique minimize the alteration of the surface by the beam. The energies of the particles are high enough to ensure that their trajectories will not be significantly altered by the ionization process. The image force acts perpendicularly to the surface and may slightly influence the polar deflection angle, although the azimuthal angle of ejection will be unaffected. For an image force of 4 eV, for example, a particle with 20-eV kinetic energy and a polar deflection angle of 45° will experience an additional 3° deflection. We also note that for clean copper exposed to 5-keV Ne⁺ ion bombardment under dynamic conditions, the angular distributions of the ions and neutrals have been found to be similar.¹⁵

This work was supported by the National Science Foundation (Grant No. MPS75-9308), the Materials Research Program (Grant No. DMR-77-23798), and the U. S. Air Force Office of Scientific Research (Grant No. AF762974). Portions of the computations were supported by the Foundation Research Program of the Naval Postgraduate School with funds provided by the Chief of Naval Research, and by the Lawrence Berkeley Laboratory supported by the U. S. Department of Energy.

^(a)J. S. Guggenheim Fellow on leave at Materials and Molecular Research Division, Lawrence Berkeley Laboratory, Berkeley, Calif. 94720 (1977-1978).

¹Over a hundred papers have appeared concerning this topic since 1956. For a review see P. Sigmund, *Rev. Roum. Phys.* **17**, 1079 (1972); C. Carter and J. S. Colligon, *Ion Bombardment of Solids* (American Elsevier, New York, 1968).

²A. L. Southern, W. R. Willis, and M. T. Robinson, *J. Appl. Phys.* **34**, 153 (1963).

³D. E. Harrison, Jr., N. S. Levy, J. P. Johnson, III, and H. M. Effron, *J. Appl. Phys.* **39**, 3742 (1968).

⁴D. E. Harrison, Jr., W. L. Moore, Jr., and H. T. Holcombe, *Radiat. Effects* **17**, 167 (1973).

⁵D. E. Harrison, Jr., and C. B. Delaplain, *J. Appl. Phys.* **47**, 2252 (1976).

⁶D. E. Harrison, Jr., P. W. Kelly, B. J. Garrison, and N. Winograd, to be published; B. J. Garrison, N. Winograd, and D. E. Harrison, Jr., to be published.

⁷R. G. Muscat and H. P. Smith, Jr., *J. Appl. Phys.* **39**, 3579 (1968).

⁸G. S. Anderson and G. K. Wehner, *J. Appl. Phys.* **31**, 2305 (1960).

⁹For the A-top case, variation of the binding energy from 0.5 to 2.0 eV does not change the main features of the patterns although the number of ejected atoms is significantly reduced for the higher binding energies. Further details of these studies and results for oxygen on a (110) and (111) orientation will be presented in a full account.

¹⁰J. Pendry, *Low Energy Electron Diffraction* (Academic, New York, 1974).

¹¹G. Apai, P. S. Wehner, R. S. Williams, J. Stohr, and D. A. Shirley, *Phys. Rev. Lett.* **37**, 1497 (1976).

¹²J. J. Czyzewski, T. E. Madey, and J. T. Yates, Jr., *Phys. Rev. Lett.* **32**, 777 (1974).

¹³W. L. Clinton, *Phys. Rev. Lett.* **39**, 965 (1977); M. L. Knotek and P. J. Feibelman, *Phys. Rev. Lett.* **40**, 964 (1978).

¹⁴A. Benninghoven, *Sur. Sci.* **53**, 596 (1975).

¹⁵V. E. Yurasova, A. A. Sysoev, G. A. Samsonov, V. M. Bukhanov, L. N. Nevzorova, and L. B. Shelyakin, *Radiat. Effects* **20**, 89 (1973).

Steady-State Vortex-Line Density in Turbulent He II Counterflow

R. M. Ostermeier, M. W. Cromar,^(a) P. Kittel,^(b) and R. J. Donnelly

Department of Physics, University of Oregon, Eugene, Oregon 97403

(Received 22 August 1978)

We have measured the steady-state vortex-line density in turbulent counterflow using a second-sound-burst technique as a local probe. Contrary to the Vinen theory and previous assumptions, we find substantial line-density inhomogeneity and strong departures from the predicted heat-current dependence. Anomalous behavior of the line density at higher heat currents provides evidence for a new secondary flow state.

In a classic series of experiments Vinen¹ was the first to study in detail the nature of turbulent counterflow in wide (~1 cm) channels. Using a

resonant second-sound technique he measured the steady-state and transient attenuation averaged over the length of the channel. On the basis